Formulation and Physical Characterization of Large Porous Particles for Inhalation

Rita Vanbever,[1,2,3] Jeffrey D. Mintzes,[2,4] Jue Wang,[2] Jacquelyn Nice,[2,4] Donghao Chen,[2,4] Richard Batycky,[4] Robert Langer,[1] and David A. Edwards[2,4,5]

Received June 3, 1999, accepted July 31, 1999

Purpose. Relatively large (>5 μm) and porous (mass density < 0.4 g/cm^3) particles present advantages for the delivery of drugs to the lungs, e.g., excellent aerosolization properties. The aim of this study was, first, to formulate such particles with excipients that are either FDA-approved for inhalation or endogenous to the lungs; and second, to compare the aerodynamic size and performance of the particles with theoretical estimates based on bulk powder measurements.

Methods. Dry powders were made of water-soluble excipients (e.g., lactose, albumin) combined with water-insoluble material (e.g., lung surfactant), using a standard single-step spray-drying process. Aerosolization properties were assessed with a Spinhaler™ device in vitro in both an Andersen cascade impactor and an Aerosizer™.

Results. By properly choosing excipient concentration and varying the spray drying parameters, a high degree of control was achieved over the physical properties of the dry powders. Mean geometric diameters ranged between 3 and 15 μm, and tap densities between 0.04 and 0.6 g/cm^3. Theoretical estimates of mass mean aerodynamic diameter (MMAD) were rationalized and calculated in terms of geometric particle diameters and bulk tap densities. Experimental values of MMAD obtained from the Aerosizer™ most closely approximated the theoretical estimates, as compared to those obtained from the Andersen cascade impactor. Particles possessing high porosity and large size, with theoretical estimates of MMAD between 1–3 μm, exhibited emitted doses as high as 96% and respirable fractions ranging up to 49% or 92%, depending on measurement technique.

Conclusions. Dry powders engineered as large and light particles, and prepared with combinations of GRAS (generally recognized as safe) excipients, may be broadly applicable to inhalation therapy.

KEY WORDS: pulmonary drug delivery; dry powder; large porous particles; excipients; aerosolization properties.

INTRODUCTION

Inhalation aerosols traditionally comprise airborn suspensions of 1–5 μm liquid or solid particles in variable states of aggregation (1–4). Since aggregation lowers the respirable fraction of an inhalation aerosol mass, an active goal of the pharmaceutical industry has been to design inhalers capable of reproducibly deaggregating aerosols, often at the expense of inhaler size and cost (1). It has been shown that by designing therapeutic aerosol particles with very low mass density (<0.4 g/cm^3), relatively large particles (>5 μm) can be successfully inspired into the lungs (5). Large porous particles aggregate less and deaggregate more easily under shear forces than smaller, non-porous particles—all other considerations equal (3–4)—hence they appear to more efficiently aerosolize from a given inhaler device than conventional therapeutic particles. In addition, since large particles (e.g., ~10 μm) are less likely to be phagocytosed than small particles (e.g., ~2 μm) (5), inhalation aerosols consisting of large porous particles appear to have a special capability to release therapeutics into the lungs over relatively long periods of time, an attribute that might be exploited by designing large porous particles of relatively low water solubility (6–8).

In this article, we report the design of a class of large porous particles for inhalation that are: 1) formed of excipients that are either FDA-approved for inhalation or endogenous to the lungs (or both); 2) relatively lipophilic with the potential for sustained release of a therapeutic; and 3) prepared by a standard, one-step pharmaceutical spray drying process. We show that theoretical estimates of mass mean aerodynamic diameter (MMAD) can be made in terms of the geometric size, as measured by Coulter multisizing, and the "sphere-envelope" mass density, as measured by tap density. We show that estimates of experimental MMAD vary depending on measurement technique, and that they most closely approximate the theoretical estimates when time-of-flight (Aerosizer™) measurements are made.

MATERIALS AND METHODS

Chemicals

β-lactose (crystalline), human serum albumin (fraction V, 96–99% albumin), DL-α-phosphatidylcholine dipalmitoyl (DPPC, synthetic, crystalline, ~99%), albuterol (hemisulfate salt), 17 β-estradiol, human insulin (recombinant expressed in Esherichia Coli, 28 USP units per mg) and sodium hydroxide were obtained from Sigma Chemical Co. (St. Louis, MO).

Solutions (0.5 or 1 L) were prepared for spray drying according to the following procedure. Water-soluble excipients and/or drug (i.e., lactose, albumin, albuterol and/or insulin) were dissolved in distilled water. To study the effect of pH on particle morphologies or to dissolve insulin, HCl (J.T. Baker) or NaOH were added to solutions. The water-insoluble excipient

[1] Department of Chemical Engineering, Massachusetts Institute of Technology, Cambridge, Massachusetts 02139.
[2] Department of Chemical Engineering, Pennsylvania State University, University Park, Pennsylvania 16802.
[3] Present address: Department of Pharmaceutical Technology, School of Pharmacy, Université catholique de Louvain, Brussels, Belgium.
[4] Present address: Advanced Inhalation Research, Inc., 840 Memorial Drive, Cambridge, Massachusetts 02139.
[5] To whom correspondence should be addressed. (e-mai: david@airpharm.com)

ABBREVIATIONS: a, radius of the particle; d, mass mean geometric diameter of the particles; DPPC, dipalmitoylphosphatidylcholine; ED, emitted dose exiting the dry powder inhaler; ε, particle porosity; **F**, force vector; **g**, gravity vector; M, mass of powder; MMADe, experimental mass median aerodynamic diameter of the particles; MMADt, theoretical mass mean aerodynamic diameter of the particles; N, number of particles in the powder; ρ, mean particle mass density; ρ_l, 1 g/cm^3; ρ_s, skeletal mass density of the particle; RF, respirable fraction of the aerosolized powder; R_p, pore radius of the particle; **u**, velocity vector; V, volume of powder; V_{part}, particle volume; V_{voids}, total volume of space between the sphere-envelope boundaries of individual particles in the powder; μ, viscosity of air; κ_o, hydraulic permeability of the porated particle.

and/or drug (i.e., DPPC and/or estradiol) were dissolved in 95 percent ethanol. The two solutions were then combined to form an 87 percent ethanolic solution of 0.1% w/v total powder concentration which was processed by spray-drying within an hour.

Spray Drying

A Niro Atomizer Portable Spray Dryer (Niro, Inc., Colombus, MD) was used to produce the dry powders. Compressed air with variable pressure (1 to 5 bar) ran a rotary atomizer (2,000 to 30,000 rpm) located above the dryer. Liquid feed with varying rate (20 to 66 mL/min) was pumped continuously by an electronic metering pump (LMI, model #A151-192s) to the atomizer. Both the inlet and outlet temperatures were measured. The inlet temperature was controlled manually; it could be varied between 100°C and 400°C and was established at 100, 110, 150, 175 or 200°C, with a limit of control of 5°C. The outlet temperature was determined by the inlet temperature and such factors as the gas and liquid feed flow rates; it varied between 50°C and 130°C. A container was tightly attached to the cyclone for collecting the powder product. Yields varied between 3 and 80% with a trend toward higher yields at lower temperatures.

Particle Size, Density and Shape

Particles of the dry powders were viewed using a conventional scanning electron microscope (SEM Model 5400, Japan Electrical Optical Laboratory, Peabody, MA) at an accelerating voltage of 20 kV. Electron micrographs were taken on a 55 Polaroid film. The mass mean particle size and size distribution of the dry powders were measured with a Coulter Multisizer II (Coulter Electronics, Luton, England) by suspending powder in an aqueous solution; these values were confirmed by inspection of electron micrographs of the particles. Bulk tap density measurements were made using a Vankel USP tap density meter (Cary, NC).

In Vitro Aerosol Deposition

Hard gelatin capsules (size 2, Eli Lilly, IN) were filled to approximately 50% with the dry powder, since half-filled capsules were shown to emit the largest amount of powder in preliminary experiments. Capsules were placed in a Spinhaler™ dry powder inhaler (Fisons, Bedford, MA) and the liberated powder drawn through an Andersen cascade impactor (1 ACFM Eight Stage Non-Viable Cascade Impactor, Graseby Andersen, Atlanta, GA) operated at a flow rate of 28.3 L/min for 10 s (9). The amount of powder deposited on each stage of the impactor was determined by measuring the difference in weight of the filters (Graseby Andersen) placed on the different trays. The "emitted dose" was determined as the percent of total particle mass exiting the capsule and the "respirable fraction" of the aerosolized powder calculated by dividing the powder mass recovered from the terminal stages (≤ cut-off aerodynamic diameter 4.7 μm) of the impactor by the total particle mass recovered in the impactor. A plot of the amount of powder deposited on each stage of the impactor against the effective cut-off diameter for that stage allowed calculation of the (experimental) mass median aerodynamic diameters (MMADe) of the particles. The use of filters for collecting powder particles on the impactor plates was validated by comparing the filter method with a method wherein each plate was coated with a viscous fluid, as recommended by the Pharmacopeia (9). No statistical difference in respirable fractions was observed between the results of the different methods.

MMADe and respirable fraction values were also assessed by aerosolization of powders in an Aerosizer™ (Amherst Process Instrument, Inc; Amherst, MA) based on direct time-of-flight measurements. The measurements were carried out in the Aero-Breather™ mode using the Spinhaler™ device, with an air flow rate of 28.3 L/min. Aerodynamic diameter was determined via the Aerosizer computational software upon evaluating time-of-particle-flight and setting the reference mass density to unity, corresponding to an assumption that the highly porous nature of the powders results in low particle Reynolds number. Specifically, time-of-flight is determined computationally by solving the force balance,

$$C_d \frac{\pi d^2}{4} \rho_a \frac{(V_a - V_p)^2}{2} = \frac{1}{6} \pi d^3 \rho_p \frac{dV_p}{dt}$$

where C_d is the particle drag coefficient, d the particle geometric diameter, ρ_a the density of air, ρ_p the density of the particle, V_a the velocity of air, and V_p the velocity of the particle. When the particle Reynolds number is small (owing to very low mass density, $V_a \sim V_p$),

$$Re_p = \frac{\rho_a (V_a - V_p) d}{\mu} << 1$$

then C_d is proportional to the inverse of the particle Reynolds number ($1/Re_p$) and

$$\left(\frac{dV_p}{dt}\right) d_a^2 = const^* \mu (V_a - V_p)$$

where $d_a = \sqrt{\rho_p} d$ is the aerodynamic diameter. Hence, in the limit of very light particles, the time of flight (underlying the magnitude of V_p) can be determined from the original force-balance equation upon setting the particle mass density to unity and interpreting the geometric diameter (d) as the aerodynamic diameter (MMADe).

Statistical Analysis

Geometric particle diameters (mean ± the standard deviation, sd, from 1 measurement) and tap densities (mean ± sd of 3 successive measurements) were measured on bulk powders. In order to study the effect of particle composition and spray drying parameters on particle diameter, density and shape, each spray drying run was reproduced 2 to 9 times. Geometric particle diameters and tap densities are expressed as average values of the different runs (± standard error of the mean, sem; Figs. 2, 4 and 5). Electron micrographs of represensative particles are shown in Fig. 3. Selected particles were analyzed for aerosolization properties, and emitted doses, respirable fractions and experimental aerodynamic diameters expressed as average values of 3 successive measurements (Fig. 6, Table I). To avoid overcrowding of Fig. 6, sd of measurements are only given in Table I. Data were analyzed by the Anova and Scheffé tests ($p < 0.05$).

Table I: Aerosolization Properties of Large Porous Particles

Drug load[a]	d (μm)	ρ (g/cm³)	MMADt (μm)	Andersen cascade impactor			Aerosizer™	
				MMADe (μm)	ED (%)	RF (%)	MMADe (μm)	RF (%)
4%A	8.8 ± 3.3	0.310 ± 0.007	4.9 ± 1.3	6.7 ± 1.5	69 ± 22	20 ± 1	5.1 ± 1.5	25
4%A	9.7 ± 4.9	0.300 ± 0.004	5.3 ± 2.1	7.5 ± 1.4	45 ± 8	16 ± 1	5.3 ± 1.5	24
4%A	10.4 ± 4.0	0.080 ± 0.006	2.9 ± 0.9	6.9 ± 1.4	79 ± 18	17 ± 2	3.3 ± 1.6	72
10%E	8.3 ± 4.5	0.087 ± 0.002	2.5 ± 1.1	5.2 ± 1.5	96 ± 6	39 ± 4	2.6 ± 1.4	92
10%E	9.1 ± 7.1	0.042 ± 0.000	1.9 ± 1.2	5.6 ± 2.5	94 ± 4	30 ± 8	2.6 ± 1.5	88
90%E	7.8 ± 3.6	0.182 ± 0.008	3.3 ± 1.2	6.7 ± 1.6	67 ± 8	25 ± 2	4.2 ± 1.5	44
90%E	9.2 ± 5.2	0.094 ± 0.003	2.8 ± 1.4	6.8 ± 1.5	84 ± 13	22 ± 2	3.2 ± 1.6	73
90%E	15.1 ± 7.3	0.082 ± 0.004	4.3 ± 2.0	7.3 ± 1.5	76 ± 11	17 ± 1	4.1 ± 1.6	47
3%I	7.7 ± 3.5	0.062 ± 0.004	1.9 ± 0.9	5.62 ± 0.02	71 ± 3	33 ± 4	3.4 ± 1.2	66
5%I	6.2 ± 3.4	0.158 ± 0.006	2.5 ± 1.4	4.78 ± 0.06	80 ± 20	49 ± 1	3.2 ± 1.5	77

[a] A, Albuterol loaded particles; E, Estradiol loaded particles; I, Insulin loaded particles. Data are presented as average values of 3 successive measurements (± standard deviation). Meaning of the acronyms is given in the Abbreviations section of the text.

RESULTS

Mass Mean Aerodynamic Diameter

Prior to discussing the preparation and characterization of porous powders for inhalation, it is useful to consider a property of the spray dried powders that is critical to evaluating their aerodynamic performance, namely the (theoretical) mass mean aerodynamic diameter (MMADt). MMADt is classically defined for *nonporous spherical* particles by (10):

$$MMADt = \sqrt{\frac{\rho}{\rho_1}}\, d \qquad (1)$$

where d is the mass-mean geometric diameter of the powder, ρ the mean particle mass density, and $\rho_1 = 1$ g/cm³. The MMADt of the particle corresponds, therefore, to the diameter of a sphere of $\rho = 1$ g/cm³ were it to fall under gravity with the same velocity. It is possible to generalize Eq. (1) for the types of highly porous, spherically-isotropic particles examined in this study, and thereby to identify the physical properties needed to estimate MMADt, by considering a spherical particle perforated by randomly oriented cylindrical pores falling under gravity (Fig. 1). As shown in Appendix A (see Eq. (A20), with $\mathbf{F} = 4/3\ \pi\rho a^3\mathbf{g}$, $2a = d$), the porous sphere will fall through air with a velocity

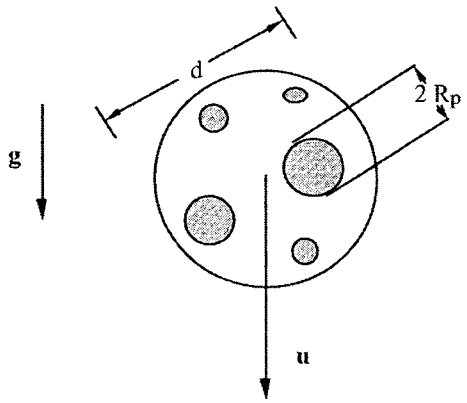

Fig. 1. Illustration of a porous particle falling under gravity. The particle of diameter, d, is permeated isotropically by cylindrical pores of radius, R_p, and falls under gravity, **g**, with a velocity **u**.

$$\mathbf{u} = \rho_s d^2 \left(\frac{1}{18\mu}\right)\left[\frac{1-\varepsilon}{1-\dfrac{1}{1+\dfrac{d^2}{18\kappa_0}}}\right]\mathbf{g} \qquad (2)$$

where ρ_s is the skeletal mass density of the particle (e.g., as measured by pycnometry), μ is the viscosity of air, ε is the particle porosity and **g** is the gravity vector. Given that the hydraulic permeability of the (cylindrically) porated particle is $\kappa_0 = \varepsilon R_p^2/8$, with R_p the pore radius (see Appendix A for clarification of these terms), Eq. (2) becomes

$$\mathbf{u} = \rho_s d^2\left(\frac{1}{18\mu}\right)(1-\varepsilon)\left[1-\frac{\varepsilon}{\varepsilon+\dfrac{16}{9}\left(\dfrac{d}{2R_p}\right)^2}\right]^{-1}\mathbf{g} \qquad (3)$$

The aerodynamic diameter of the porous sphere can now be calculated by comparing Eq. (3) with the related formula for a *nonporous sphere* of unit mass density (ρ_1), i.e.,

$$\mathbf{u} = \rho_1\, MMADt^2\left(\frac{1}{18\mu}\right)\mathbf{g} \qquad (4)$$

which shows that

$$MMADt = d\left[\frac{\dfrac{\rho_s(1-\varepsilon)}{\rho_1}}{1-\dfrac{\varepsilon}{\varepsilon+\dfrac{16}{9}\left(\dfrac{d}{2R_p}\right)^2}}\right]^{1/2} \qquad (5)$$

This relationship simplifies upon noting that for pore sizes relatively small compared to the particle diameter itself ($d/2R_p \geq 3$),

$$MMADt \cong d\sqrt{\frac{\rho_s(1-\varepsilon)}{\rho_1}} \qquad (6)$$

Finally, comparison of Eqs. (1) and (6) reveals that, for porous

particles of approximately spherical shape, with pore sizes as large as approximately 1/3 the diameter of the particles themselves, the appropriate measure of particle mass density ρ (as appears in Eq. (1)) is

$$\rho \cong \rho_s(1 - \varepsilon) \tag{7}$$

This relationship is explicitly independent of pore radius, as well as the limiting assumption of the simple geometrical pore model. That is, the particle falls under gravity with a velocity that is proportional to the net mass enclosed in the sphere envelope diameter d, as is physically intuitive.

An approximate bulk measure of ρ as defined by Eq. (7), is provided by the tap density. In tap density experiments a mass (M) of powder is tightly filled into a volume (V), and the ratio *M/V* used to approximate ρ. The mass M can be expressed as

$$M = \sum_{n=1}^{N} \frac{4}{3}\pi\left(\frac{d_n}{2}\right)^3 \rho_{sn}(1 - \varepsilon_n) \tag{8}$$

where N is the number of particles in the powder. The volume V is given by

$$V = \sum_{n=1}^{N} \frac{4}{3}\pi\left(\frac{d_n}{2}\right)^3 + V_{\text{voids}} \tag{9}$$

where the first term on the right side of Eq. (9) denotes the particle volume (V_{part}), i.e., $V_{\text{part}} = \sum_{n=1}^{N} 4/3\ \pi(d_n/2)^3$, and V_{voids} denotes the total volume of space between the sphere-envelope boundaries of individual particles in the powder. Dividing Eq. (8) by (9) gives

$$\frac{M}{V} = \rho_s(1 - \varepsilon)\left[\frac{1}{1 + \dfrac{V_{\text{voids}}}{V_{\text{part}}}}\right] \tag{10}$$

where

$$\rho = \rho_s(1 - \varepsilon) = \frac{\sum_{n=1}^{N} \frac{4}{3}\pi\left(\frac{d_n}{2}\right)^3 \rho_{sn}(1 - \varepsilon_n)}{\sum_{n=1}^{N} \frac{4}{3}\pi\left(\frac{d_n}{2}\right)^3} \tag{11}$$

is the mean mass density of the powder. The ratio $V_{\text{voids}}/V_{\text{part}}$ can be roughly estimated by assuming an efficient packing of a monodisperse assay of spheres; this gives $V_{\text{voids}}/V_{\text{part}} = 0.2595$ (11), resulting in

$$\frac{M}{V} = \rho_s(1 - \varepsilon)\left(\frac{1}{1 + 0.2595}\right) = 0794\rho_s(1 - \varepsilon) \tag{12}$$

Comparing Eqs. (12) and (7) shows that the relationship between the tap density (*M/V*) and the "particle density" of interest in the evaluation of MMADt for porous particles, is

$$\frac{M}{V} = 0.794\rho \tag{13}$$

meaning that the tap density is approximately a 21% underestimate of the 'true' density $\rho_s(1 - \varepsilon)$. In real scenarios, polydispersity of powders reduces the amount of void space in a packed powder, as does interlocking of particles, whereas conventional tapping density measurements may result in less than perfect packing. These counterbalancing effects suggest that tap density estimates of ρ, for use in Eq. (1), may remain approximately a 20% systematic underestimate of actual values.

In the remainder of this article, theoretical estimates of aerodynamic diameter (MMADt) are made using Coulter Counter diameters to estimate d, and tap density values to estimate ρ. We compare theoretical values (MMADt) with experimental values (MMADe) in a later subsection.

Formation of Large Porous Particles

The effects of powder composition, solution properties and spray drying parameters on the geometrical properties of the spray dried powders were examined in our experimental study. Powder composition most greatly affected particle size, density and morphology. As shown in Fig. 2, a maximum particle size and minimum particle density occurred at 60% DPPC concentration (Anova and Scheffé tests, $p < 0.05$). DPPC concentration had an important impact on particle shape as well, with increasing DPPC content transforming particle morphology from torroidal (0% and 30% DPPC), to sponge-like (60% DPPC), to spherical (90% DPPC) (Fig. 3). These three particle configurations were also the main types encountered in our experiments. In general, adding lactose led to smaller and heavier particles, while adding albumin contributed to larger and lighter particles. Albumin appeared also responsible for the sponge-like shape of the particles, whereas lactose tended to produce spherical shapes.

The pH of the feed solution significantly influenced particle density (Anova, $p < 0.05$) and morphology, although an effect on particle size was also observed (Anova, $p < 0.05$). Prior to mixing with ethanol, decreasing the pH of the aqueous solution from 7 to 4 increased the density 3-fold for albumin/lactose/DPPC (20/20/60 w/w/w) particles while decreasing their size by a factor of 1.5 (Scheffé test, $p < 0.05$; Fig. 4). A similar trend was observed when increasing the pH from 7 to 10 (Scheffé test, $p < 0.05$; Fig. 4). A sponge-like shape was observed at pH 7, but partially lost at the lower and higher pH values examined (data not shown).

Spray drying parameters affected particle characteristics as well. Inlet temperature had an especially important impact on particle morphology. Increasing the temperature from 110°C

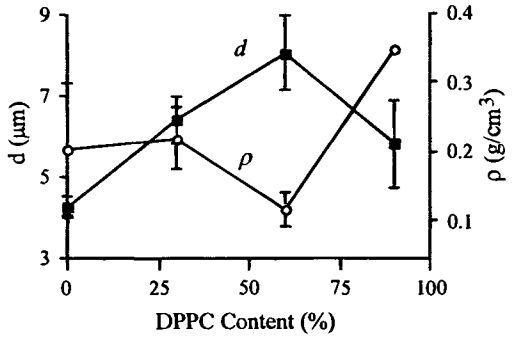

Fig. 2. Influence of DPPC content on particle diameter, d (■), and density, ρ (○). The powders were made of variable DPPC content with lactose and albumin present in equivalent amounts. Spray drying was carried out with an inlet temperature of 110°C, a feed rate of 40 mL/min and a spin rate of 17,000 rpm.

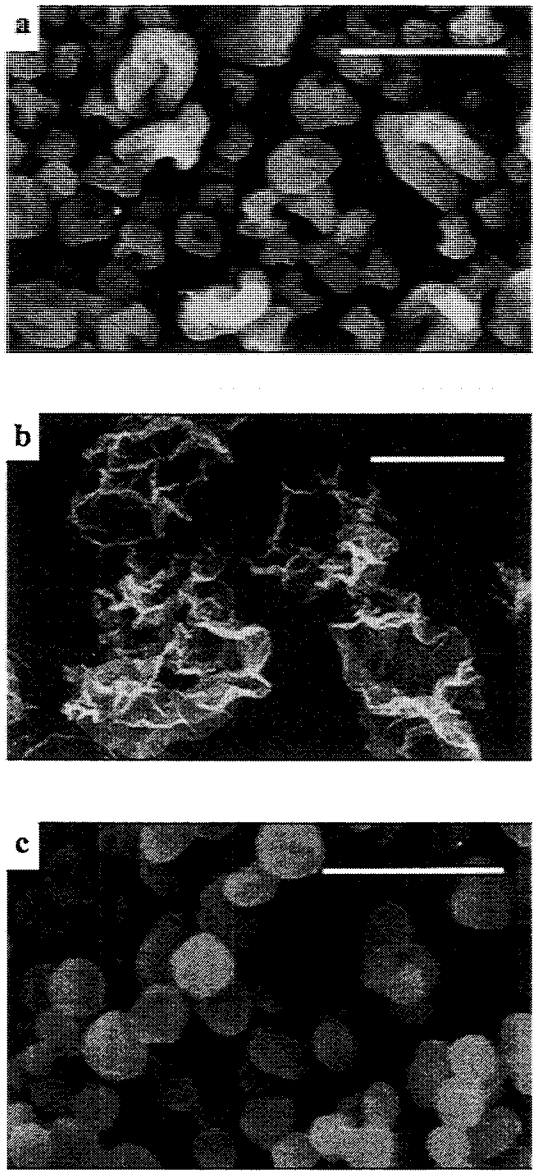

Fig. 3. Impact of DPPC content on particle shape. Increasing DPPC content transformed particle morphology from torroidal and sponge-like (30% DPPC, **a**), to sponge-like (60% DPPC, **b**), to spherical (90% DPPC, **c**). These particle types were the mains encountered in our experiments. Scanning electron microscope images of particles presented in Figure 2 for size and density are shown. Scale bars are 10 μm.

to 175°C changed particle morphology from an extremely high surface area sponge-like shape to a low surface area torroidal shape (data not shown). Increasing the temperature also decreased particle size (Anova, $p < 0.05$) while tending to increase particle density (Anova, $p > 0.05$; Fig. 5).

As described elsewhere (12–13), increasing the solution feed rate and/or decreasing the atomizer spin rate increased the size of the particles and broadened their size distribution. These two parameters had no evident effect on mass density and particle morphology (data not shown).

Among the formulations and conditions tested, the albumin/lactose/DPPC (20/20/60 w/w/w) formulation described in Figs. 2, 3 and 4 appeared to exhibit especially large size, low

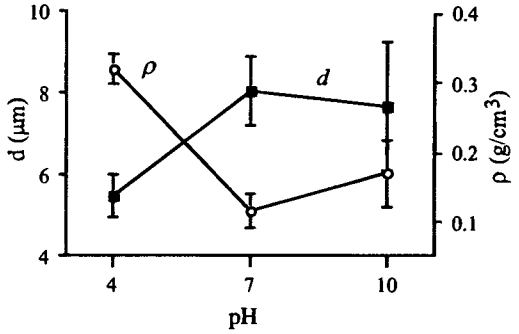

Fig. 4. Influence of the pH of the feed solution on particle diameter, d (■), and density, ρ (○). The particles were made of albumin/lactose/DPPC 20/20/60 w/w/w at an inlet temperature of 110°C, a feed rate of 40 mL/min and a spin rate of 17,000 rpm.

bulk density and MMADt in the range 1–3 μm. We incorporated albuterol sulfate (at 4% particle load) and estradiol (at 10% particle load) into these particles (Table I). In the case of albuterol sulfate, this involved formation of particles with composition albumin/lactose/DPPC/albuterol sulfate (18/18/60/4 w/w/w/w). For delivery of a standard human dose of 200 μg, this loading requires delivery to the lungs of 5 mg of powder, an amount easily achievable using a capsule-based inhaler such as the Spinhaler™. In the case of estradiol, drug loading involved formation of particle compositions albumin/lactose/DPPC/estradiol (15/15/60/10 w/w/w/w). For delivery of a standard (long-acting) human dose of 300–500 μg, this loading requires delivery to the lungs of 6 mg of powder, a powder mass again easily achievable using a Spinhaler™ (or similar capsule) inhaler device (17). In both cases, drug loading did not significantly alter the physical characteristics of the powders. Also, in both cases, the large fraction of insoluble lipid material led to sustained-release of the drug in vivo (6–7). Particles incorporating insulin were also prepared. Due to the acid used for dissolving insulin and excipients, largest and lightest particles were obtained with albumin/DPPC 40/60 w/w, and no lactose (Fig. 4; see 8). A load of insulin up to 5% did not induce alteration of physical properties of those powders. Finally, to evaluate the ability to prepare highly porous powders with high drug loading by spray drying, we also prepared 90% estradiol (10% DPPC) powders. These had mean size near 10μm and

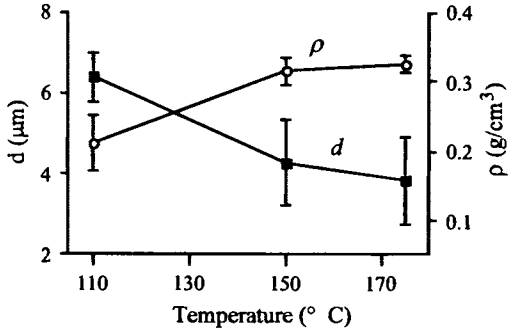

Fig. 5. Influence of the inlet temperature on particle diameter, d (■), and density, ρ (○). The particles were made of albumin/lactose/DPPC 33/33/33 w/w/w at varying inlet temperature, a feed rate of 40 mL/min and a spin rate of 17,000 rpm.

bulk tap densities near or below 0.1 g/cm^3, as shown in Table I, and subsequently discussed in Fig. 6 (see 7).

Aerosolization Properties of Large Porous Particles

The aerosolization properties of porous particles were evaluated with lactose/albumin/DPPC formulations, incorporating albuterol sulfate, estradiol or insulin. To vary MMADt in the range 1–5 μm, while keeping mean particle size large (greater than approximately 6 μm), we varied the spray drying parameters using the variables described above. We then measured the mean particle size (d) and mass density (ρ) of the powders, and calculated theoretical aerodynamic diameters (MMADt) based on Eq. (1). These values are listed in Table I. Using the Spinhaler™ device with both the Andersen cascade impactor and Aerosizer™, we measured the aerodynamic properties of the powders. Figure 6a shows the trend of emitted dose (ED) from the Spinhaler™ device versus MMADt. The large porous particles generally aerosolize effectively from the Spinhaler™ device over the entire range of MMADt, with the powders possessing MMADt ≤ 2 μm showing especially good aerosolization (ED up to 96%). Increased ED with decreased MMADt owes to decreased ρ at low MMADt (Table I). Figure 6b shows a stronger correlation between aerosolization properties and MMADt, where respirable fraction (RF) values generally increase with decreasing MMADt. The variability in ED and RF observed for similar MMADt may be caused by different powder compositions (e.g., some powders are made principally of estradiol), densities and sizes, as well as by variabilities inherent to the methods for measuring aerosolization properties (see Table I, 14). Interestingly, the RF values measured by the Aerosizer™ are consistently greater than those measured by the Andersen impactor. This corresponds to significantly different experimental estimates of MMAD (Table I), with MMADe values assessed by means of the Aerosizer™ being much nearer the theoretical estimates, as shown in Fig. 6c.

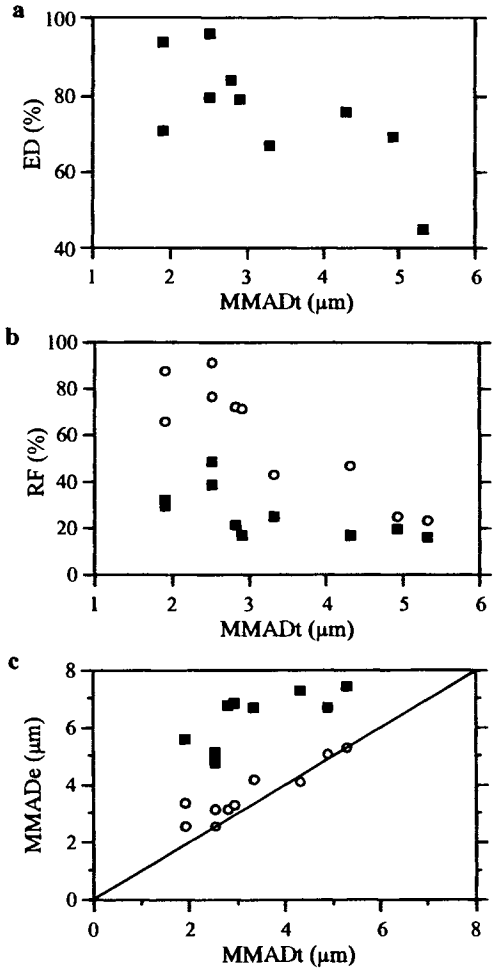

Fig. 6. Aerosolization properties of porous particles. a. Emitted dose, ED, versus theoretical mass mean aerodynamic diameter, MMADt. b. Respirable fraction, RF, versus MMADt, as measured with the Andersen cascade impactor (■) and Aerosizer™ (○). c. Experimental mass median aerodynamic diameter, MMADe, versus MMADt, as measured with the Andersen cascade impactor (■) and Aerosizer™ (○).

DISCUSSION

Dry powders engineered as large and light particles, and prepared with combinations of GRAS (Generally Recognized As Safe) excipients may be broadly applicable to inhalation therapy. The powders are shown to aerosolize efficiently from a standard dry powder inhaler, exhibit elevated respirable fractions, and can provide sustained drug release in the lungs through the use of lipophilic components (Table I, Fig. 6; 5–8).

The aerosolization properties of the porous powders are particularly optimal for MMADt values less than 3μm (Table I, Fig. 6). When aerosolized from the Spinhaler™ device at 28.3 L/min (a flow rate at which the Spinhaler™ performs suboptimally; 15) porous powders with MMADt < 3 μm exhibit ED values up to 96%, a strikingly high ED value (Fig. 6a). As shown in Table I, high ED values are related to low particle mass densities, which underlines the importance of lowering gravitational and inertial forces for efficient aerosolization (3). Of the aerosolized powder, the mass fraction of powder capable of penetrating the peripheral airways (MMADt < 4.7 μm) is also high for MMADt < 3 μm, with values ranging up to 49–92% depending on method of assessement (Fig. 6b). These high values suggest that large porous particles may be very attractive for inhalation therapy.

The poor agreement between Andersen-impactor and Aerosizer™ collected respirable fractions (RF) and measured MMADe may underly the fact that mechanisms of transport and deposition of large porous particles involved in the methods are not the same, hence these methods may have differing relevance to the situation in vivo (Figs. 6b and c). The major deposition processes of particles in human airways are: 1) inertial impaction, which is dominant in the upper airways where velocities are maximum, 2) sedimentation, which is predominant throughout the central and distal tract and 3) diffusion, which is most important for submicrometer-size particles (1,15). Since porous particles experience less lubrication-layer repulsion than small nonporous particles of similar aerodynamic size, deposition by inertial impaction in the Andersen impactor (and possibly in the upper airways) may increase. That is, the Andersen impactor depends on an indirect relationship between particle aerodynamic size and stage of the impactor and it is possible that this relationship is altered for particles that are much lighter and correspondingly larger than those used for the impactor calibration; in other words, the impactor may

separate particles not exclusively based on aerodynamic size, but by some combination of aerodynamic and geometric sizes. Higher deposition in the early stages of the Andersen impactor would lead to underestimates of RF and overestimates of MMAD. On the other hand, the Aerosizer™, by measuring directly the time of particle flight, can give, in principle, a direct measurement of aerodynamic size (see Fig. 6c). While more work need to be done to clarify the relevance of these results to in vivo performance, recent scintigraphy results in humans with large porous particles have shown that particles of geometric size 10 μm and aerodynamic size (as measured by the Aerosizer™) near 3 μm can deposit with greater than 60% efficiency in the lungs (26).

The preparation of large light particles by spray drying appears to be governed by similar rules as have been previously established for particulate spray drying in general (12). In particular, the effects of spray drying parameters on particle size and shape indicated in Figs. 2–5 are well documented in the literature (e.g., 12,16–17). The effect of pH on particle characteristics (Fig. 4) is however noteworthy, as a change in pH is often used to dissolve compounds. By changing the pH from 4 to 7 to 10, albumin (pI = 4.9) changed from positively to negatively charged. The change in the electrical charge of albumin and consequently the alteration of the intermolecular interactions may explain the changes in particle characteristics observed at different pH values. Similarly, the size of albumin microspheres prepared using high-speed homogenization and subsequent heat denaturation was shown to be strongly affected by the pH of the albumin solution (18–19).

Of special interest to the preparation of porous powders by spray drying is the approximate constancy of overall particle mass with varying composition, pH and inlet temperature. When the particle size increases, the mass density in general decreases in such a way that the overall particle mass remains in the same order of magnitude (Figs. 2, 4 and 5). This phenomenon apparently reflects the fact that primary droplet mass produced by the spray drying process is not strongly affected by changes in these process parameters. Thus, temperature, pH and composition may impact on the evaporation/condensation process, but do not strongly impact on overall particle mass (12–13).

The use of albumin and DPPC in the powders facilitates porous particle formation and/or long particle life (Figs. 2–3). Both excipients appear to be logical candidates for inhalation, especially as they are present in abundant concentrations in the lungs (20–21). The use of DPPC or albumin in the aerosols should not lead to significant accumulation of these endogenous materials in the lungs following chronic daily administration. Specifically, assuming a daily dose of 5 mg of powder, a fine particle fraction of 40% (Fig. 6b) and an average percentage of DPPC and/or albumin in the powder of 50% by weight, the amount of DPPC or albumin added in the alveoli every day would only be approximately 1 mg. Given the clearance rate of the epithelial lining fluid and the endogenous levels of DPPC and albumin within this fluid, chronic administration would not add more than 3% to the quantities of DPPC and albumin eliminated every day from the lungs (22; Appendix B).

APPENDIX A: STOKES DRAG ON A TRANSLATING POROUS SPHERE

Consider a sphere of radius a permeated isotropically by cylindrical pores of radius R_p, with porosity ε. The sphere translates through an unbounded fluid with velocity $\mathbf{u}$ under a force $\mathbf{F}$ (Fig. 1). The Stokes flow around the sphere can be described by the equations

$$\mu\nabla^2\mathbf{v} = \nabla p \tag{A1}$$

$$\nabla \cdot \mathbf{v} = 0 \tag{A2}$$

in the fluid, with boundary condition

$$\mathbf{v} = \mathbf{u}(1 - \kappa) \ @ \ r = 0 \tag{A3}$$

at the sphere surface, and

$$(\mathbf{v}, p) \rightarrow (0, p_\infty) \ @ \ r \rightarrow \infty \tag{A4}$$

far from the sphere. The constant κ reflects the permeability of the sphere in a manner yet to be determined. Due to the linearity of the problem, we introduce

$$\mathbf{v} = \mathbf{V} \cdot \mathbf{u} \tag{A5}$$

$$p - p_\infty = \mu\Pi \cdot \mathbf{u} \tag{A6}$$

where $\mathbf{V}$ and π are functions whose solutions follow from:

$$\nabla^2\mathbf{V} = \nabla\Pi \tag{A7}$$

$$\nabla\mathbf{V} = 0 \tag{A8}$$

$$\mathbf{V} = \mathbf{I}(1 - \kappa) \ @ \ r = 0 \tag{A9}$$

$$(\mathbf{V},\Pi) \rightarrow (0,0) \ @ \ r \rightarrow \infty \tag{A10}$$

The Eq. (A7)–(A10) may be solved to give

$$\mathbf{V} = \frac{3}{4}(1-\kappa)\left(\frac{a}{r}\right)(\mathbf{I} + \mathbf{i}_r\mathbf{i}_r) + \left(\frac{1+\kappa}{4}\right)\left(\frac{a}{r}\right)^3(\mathbf{I} - 3\mathbf{i}_r\mathbf{i}_r) \tag{A11}$$

$$\Pi = \frac{3}{2}\left(\frac{1-\kappa}{a}\right)\left(\frac{a}{r}\right)^2\mathbf{i}_r \tag{A12}$$

The hydrodynamic force acting on the translating sphere is described by

$$F = \int_s \mathbf{n} \cdot \mathbf{P}dA \tag{A13}$$

where $\mathbf{n} = \mathbf{i}_r$, s is the surface area, and

$$\mathbf{P} = p\mathbf{I} + \mu(\nabla\mathbf{v} + \nabla\mathbf{v}_t) \tag{A14}$$

is the pressure dyadic. Evaluating the above eventually gives

$$\mathbf{F} = -6\pi\mu a(\kappa - 1)\mathbf{u} \tag{A15}$$

The velocity permeating the sphere as it translates is, from Eq. (A3),

$$\mathbf{v}_s = \kappa\mathbf{u} \tag{A16}$$

where "s" signifies the "seepage" velocity. This velocity is, according to Darcy's law,

$$\mathbf{v}_s = \frac{1}{\mu}\kappa_0\overline{\nabla\mathbf{p}} \tag{A17}$$

where κ_0 is the Darcy hydraulic permeability and $\overline{\nabla\mathbf{p}}$ the macroscopic pressure gradient acting over the sphere. The latter is related to the aerodynamic force by

$$\mathbf{F} = -\frac{4}{3}\pi a^3 \overline{\nabla \mathbf{p}} \tag{A18}$$

Using Eqs. (A15–A18) then gives, following manipulations,

$$\kappa = \frac{1}{1 + \frac{2}{9}\frac{a^2}{\kappa_0}} \tag{A19}$$

This allows Eq. (A15) to be recast as

$$\mathbf{F} = -6\pi\mu a\left(\frac{1}{1 + \frac{2}{9}\frac{a^2}{\kappa_0}} - 1\right)\mathbf{u} \tag{A20}$$

APPENDIX B: DOSING OF DPPC AND ALBUMIN IN THE LUNGS

Of the approximately 100 m^2 of surface area in the lungs (23) over 99.9 % is located in the respiratory bronchiole and alveolar regions (24). As the epithelial layer of the distal regions of the lungs is coated with a surfactant layer of approximately 0.1 μm thickness (24), it raises the total volume of fluid (V) in the lungs to approximately 10 mL. This entire volume of fluid is swept out of the lungs via the trachea each day (24).

The concentration of surfactant in the epithelial lining fluid is approximately 10 mg/mL (25). Given that approximately 45% of lung surfactant is DPPC (20), it translates into a total approximate mass of DPPC in the lungs of 45 mg. The epithelial lining fluid also contains albumin. Albumin concentration in the lungs is approximately 3.7 mg/mL (21), which translates into a total mass of albumin in the lungs of 37 mg.

ACKNOWLEDGMENTS

We thank Lloyd Johnston for helpful discussions. R. Vanbever was supported by a Fulbright Grant-In-Aid, a postdoctoral fellowship for scientific research from Université catholique de Louvain (UCL, Belgium) and a fellowship from the Patrimoine de la Faculté de Médecine of UCL. J. Wang was supported by a Penn State Life Science Consortium scholarship. This work was funded in part by a NSF CAREER Award (DE).

REFERENCES

1. A. J. Hickey (ed.). *Inhalation aerosols—Physical and biological basis for therapy*, in Lung Biology in Health and Disease, C. Lenfant (ex. ed.) **94**, 1996.
2. M. P. Timsina, G. P. Martin, C. Marriot, D. Ganderton, and M. Yianneskis. Drug delivery to the respiratory tract using dry powders inhalers. *Int. J. Pharm.* **101**:1–13 (1994).
3. D. L. French, D. A. Edwards, and R. W. Niven. The influence of formulation on emission, deaggregation and deposition of dry powders for inhalation. *J. Aerosol Sci.* **27**:769–783 (1996).
4. W.-I. Li, M. Perzl, J. Heyder, R. Langer, J. D. Brain, K.-H. Englmeier, R. W. Niven, and D. A. Edwards. Aerodynamics and aerosol particle deaggregation phenomena in model oral-pharyngeal cavities. *J. Aerosol Sci.* **27**:1269–1286 (1996).
5. D. A. Edwards, J. Hanes, G. Caponetti, J. Hrkach, A. Ben-Jebria, M. L. Eskew, J. D. Mintzes, D. Deaver, N. Lotan, and R. Langer. Large porous particles for pulmonary drug delivery. *Science* **276**:1868–1871 (1997).
6. A. Ben-Jebria, D. Chen, M.-L. Eskew, R. Vanbever, R. Langer, and D. A. Edwards. Inhalation of large porous albuterol particles for sustained bronchodilation. *Pharm. Res.* **16**:555–561 (1999).
7. J. Wang, A. Ben-Jebria, and D. A. Edwards. Inhalation of estradiol for sustained systemic delivery *J. Aerosol Med.* **12**:27–32 (1999).
8. R. Vanbever, A. Ben-Jebria, J. D. Mintzes, R. Langer, and D. A. Edwards. Sustained-release of insulin from insoluble inhaled particles. *Intern. Symp. Control. Rel. Bioact. Mater.* **25**:261–262 (1998).
9. *European Pharmacopoeia*, 3rd edition, addendum 1999, 74–77.
10. I. Gonda. *Topics in Pharmaceutical Sciences 1991*, D. J. A. Crommelin and K. K. Midha (eds), Medpharm Scientific, Stuttgart, 1992.
11. H. Brenner and D. A. Edwards, *Macrotransport Processes*, Butterworth-Heinemann, 1993.
12. K. Masters *Spray drying handbook* (5th. ed.), Longman Scientific and Technical, 1991.
13. M. Sacchetti and M. M. Van Oort. Spray-drying and supercritical fluid particle generation techniques. In: A. J. Hickey (ed), *Inhalation Aerosols*, Marcel Dekker, 1996, 337–384.
14. J. D. Andya, Y.-F. Maa, H. R. Costantino, P.-A. Nguyen, N. Dasovich, T. D. Sweeney, C. C. Hsu, and S. J. Shire. The effect of formulation excipients on protein stability and aerosol performance of spray-dried powders of a recombinant humanized anti-IgE monoclonal antibody. *Pharm. Res.* **16**:350–358 (1999).
15. A. R. Clark and M. Egan. Modelling and deposition of inhaled powders drug aerosols. *J. Aerosols Sci.* **25**:175–186 (1994).
16. E. Mathiowitz, H. Bernstein, S. Giannos, P. Dor, T. Turek, and R. Langer. Polyanhydride microspheres. IV. Morphology and characterization of systems made by spray drying, *J. Appl. Poly. Sci.* **45**:125–134 (1992).
17. Y.-F. Maa, P.-A. Nguyen, and S. W. Hsu. Spray drying of air-liquid interface sensitive recombinant human growth hormone. *J. Pharm. Sci.* **87**:152–159 (1998).
18. X. M. Zeng, G. P. Martin, and C. Marriot. Albumin microspheres as a means of drug delivery to the lung: analysis of the effects of process variables on particle sizes using factorial design methodology. *Int. J. Pharm.* **107**:205–210 (1994).
19. X. M. Zeng, G. P. Martin, and C. Marriot. Tetrandrine delivery to the lung: The optimisation of albumin microspheres preparation by central composite design, *Int. J. Pharm.* **109**:135–145 (1994).
20. J. A. Clements and R. J. King. Composition of the surface active material. In: R. G. Crystal (ed.), *The Biochemical Basis of Pulmonary Function*, Marcel Dekker, Inc, 1976, chap 10.
21. S. I. Rennard, G. Basset, D. Lecossier, K. M. O'Donnell, P. Pinkston, P. G. Martin, and R. G. Crystal. Estimation of volume of epithelial lining fluid recovered by lavage using urea as marker of dilution. *J. Appl. Physiol.* **60**:532–538 (1986).
22. N. J. Toremalm. The daily amount of tracheo-bronchial secretions in man. *Acta Oto-laryng.* (suppl.) **158**:43–53 (1960).
23. J. S. Patton. Mechanisms of macromolecule absorption by the lungs. *Adv. Drug Del Rev.* **19**:3–36 (1996).
24. E. R. Weibel. *Morphometry of the Human Lung*, New York Academic Press, 1963.
25. R. J. Mason and M. C. Williams. Alveolar type II cells. In: R. G. Crystal, J. R. West *et al* (eds), *The lung: scientific foundations*, New York Raven Press Ltd, 1991, Chap. 3.1.9.
26. G. Scheuch, T. Meyer, K. Sommerer, H. Lichte, A. Pohner, W. Hess, P. Brand, G. Caponetti, K. Haussinger, J. Heyder, R. Batycky, R. Niven, and D. A. Edwards. Measuring in vivo deposition of large porous particles. Presented at the Biannual ISAM Meeting, Vienna, June 12–16, 1999).